NOTES

Application of a Numerical Mesoscale Model for the Evaluation of Seasonal Persistent Regional Climatological Patterns

M. SEGAL

Department of Atmospheric Science, Colorado State University, Fort Collins 80523

Y. MAHRER

Hebrew University of Jerusalem, Levi Eshkol School of Agriculture, Rehovot 76100, Israel

R. A. PIELKE

Department of Atmospheric Science, Colorado State University, Fort Collins 80523

16 March 1982 and 18 June 1982

ABSTRACT

A three-dimensional numerical mesoscale model has been applied over the irregular terrain of northern Israel in order to simulate the local surface climate pattern associated with typical July stagnate synoptic meteorological conditions. Comparison of model-evaluated surface flow and temperature fields against observed data illustrate the role in which mesoscale models can be used in order to provide additional insight into the analyses of persistent regional climatological patterns.

1. Introduction

A common approach for regional climatological studies is based on the statistical processing of observed data, followed by a contoured interpolation of the meteorological fields of interest onto geographic maps. The accuracy of the climatological analysis depends on the spatial density of the data, as well as the amount of consideration given to the presence of such irregular terrain features as elevated topography and land-water boundaries. In situations where climatological patterns are of seasonal (or monthly) persistence, using meteorological data for typical individual days can provide a reasonable estimate of climatological patterns for the entire season (or month). Such quasi-steady conditions are prevalent at a number of geographic locations, including, for example, during the summer along the eastern and southern Mediterranean coasts (*Atlas of Israel*, 1970; Griffiths and Soliman, 1972) and along the southern coasts of California (*Climates of the States*, 1974).

Using a numerical mesoscale model to simulate such climatological conditions has the advantage of providing additional resolution when the observational data are sparse, as well as suggesting a preliminary evaluation of spatial and diurnal variations in a region where no data are available for climatological analyses. Such an approach was also reflected in Nickerson's (1979) study of the cloudiness and convergence zones over Hawaii during the summer. It is the purpose of the present note to discuss the use of a mesoscale model in this fashion, using the highly persistent surface climatology of northern Israel during the summer as an example.

In the present study, a three-dimensional numerical mesoscale model has been applied to simulate typical July conditions over that region. A similar type of simulation was previously performed by Anthes and Warner (1978). Their study provided the first modelling insight into the terrain-induced flows within the planetary boundary layer (PBL) over this region. However, that study did not simulate the prevalent synoptic flow over the region, nor was it oriented toward resolving the surface climatological patterns. In the current study, predicted surface flow patterns have been compared with those obtained by observational studies, while the predicted surface temperature fields have been verified against climatological data. The complex terrain of the region, in addition to the reasonably large amount of observational data available for wind and temperature in the simulated domain, have provided, to a large extent, a reliable situation in which to evaluate the model skill at simulating the observed spatial and diurnal variations of these climatological variables.

2. The simulated domain

Fig. 1 illustrates the simulated domain and the main terrain features. The water bodies present in the

0021-8952/82/111754-09$06.25

region include the Mediterranean Sea to the west, the Sea of Galilee (−212 m MSL), and the Dead Sea (−400 m MSL) along the Jordan Rift Valley (JRV). The mountainous areas include the Judean Mountains with typical heights above 800 m, the Galilee Mountains to the north with peaks above 900 m, and the Carmel Ridge with highest elevations of about 400 m. Along the eastern side of the JRV the mountains range from several hundred meters, to more than 1000 m at the northeastern corner of the domain.

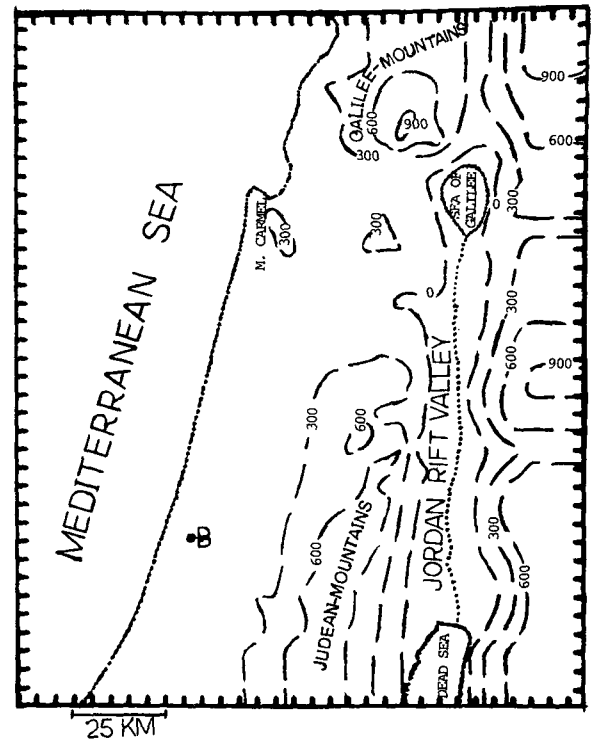

FIG. 1. Illustration of simulated domain.

3. Summer synoptic conditions

During most of the summer a permanent subtropical ridge dominates the upper atmosphere of the region. The synoptic surface conditions are characterized by a persistent trough which extends from the monsoon depression located over northern India [see Skibin and Hod (1979, Fig. 1) for a schematic illustration]. This low-level pressure field generates a highly persistent west to northwesterly gradient synoptic wind. Coupling of the sea and land breezes and mountain-induced thermal flows with the synoptic flow, leads to well-marked diurnal surface wind cycles (Skibin and Hod, 1979). Also, temperatures have a typical daily cycle of change (*Atlas of Israel*, 1970).

4. Model aspects

The numerical mesoscale model formulations are described in Pielke (1974) and Mahrer and Pielke (1978) so that in this note only a brief description of the model is given.

a. Boundary layer

The calculation of the surface fluxes of momentum, heat and moisture are based on work of Businger *et al.* (1971). The exchange coefficients in the PBL above the surface layer utilizes O'Brien's (1970) functional form. The planetary boundary layer is predicted as a function of location according to Deardorff's (1974) prognostic equation. The roughness parameter over the water is calculated according to the formula given by Clarke (1970).

b. Surface heat balance

The temperature at the soil-air interface is calculated using a heat balance equation which includes solar radiation, incoming atmospheric longwave radiation, latent, sensible and soil heat fluxes, and the outgoing surface longwave radiation.

c. Radiation

The changes of air temperature, due to shortwave and longwave radiative flux divergence, are parameterized following the methods of Atwater and Brown (1974) and Sasamori (1972). Heating of the atmosphere by shortwave radiation is confined to water vapor, while carbon dioxide and water vapor are considered in the longwave radiation heating-cooling algorithm.

d. Initial and boundary conditions

The initial atmospheric data for the model are the wind velocity, temperature and moisture. The initial wind velocity above the initial specified PBL is geostrophically balanced; within the PBL winds are determined by assuming a balance of the shear stress, the Coriolis and the pressure gradient forces. When topography is included, a dynamic initialization of the meteorological fields precedes the beginning of the simulation. Zero gradient boundary conditions are assumed at the model lateral boundaries.

e. Computational aspects

The numerical schemes are described in detail in Mahrer and Pielke (1978). The advective terms are solved by using a cubic spline technique. A modification of the Crank-Nicholson scheme as suggested by Paegle *et al.* (1976) is adopted for the diffusion terms.

In the current study, we use a horizontal grid in-

terval of 5 km (which was extended to 10, 20 and 40 km in the three grid intervals near the boundaries in order to remove the boundaries from the domain of interest), along with a time step of 90 s. Initial conditions, given in Table 1, are based on July averaged Beer Ya'aqov (B in Fig. 1) radiosonde data (Shaia, 1962), with some refinements for the vertical moisture and temperature profiles, based on the average Bet-Dagan (located near Beer Ya'aqov) radiosonde sounding. The surface parameters and boundary conditions, as given in Mahrer and Pielke (1977), are adopted in the present study. Starting at 2000 LST (following sunset) the model is integrated for the next 24 h. Test simulations with the two-dimensional version of the model for 48 h indicated that a reasonable steady-state daily cycle is established, a short period after the beginning of the simulation.

TABLE 1. Initial conditions for the simulation.

Level height (m)	Wind direction (deg)	Wind speed ($m\ s^{-1}$)	Temperature (°C)	Specific humidity ($g\ kg^{-1}$)
5	280	2.0	26.1	17.2
15	280	2.2	26.4	17.0
50	290	2.6	26.4	16.9
100	290	2.8	26.0	16.6
300	290	3.0	24.3	14.5
500	290	3.5	22.5	13.5
700	290	4.5	20.9	10.0
900	290	4.5	21.2	8.3
1200	290	4.5	20.6	6.8
1500	290	5.0	19.6	5.1
2000	270	5.0	17.8	4.3
3000	250	6.0	14.2	2.2
5000	250	8.0	2.3	1.2
7000	250	8.0	−10.6	0.5

5. Results

a. Flow patterns

The model-calculated July flow patterns for several selected hours have been compared with those obtained by two observationally oriented analyses. The first one is taken from Skibin and Hod (1979) who carried out a subjective streamline analysis for July. Their analysis is based on 41 stations which are reported to have a high degree of steadiness[1] of the wind, along with 32 additional stations with partial wind information [for station locations see Skibin and Hod (1979, Fig. 4)]. This analysis was guided by using the monthly averaged wind velocities at these stations, with terrain effects considered subjectively in the interpolations for the streamlines. The second analysis has been done by Doron (1979), who used 40 stations (their locations are marked on the figures by dark circles), and applied an inverse-square-distance, objective analysis scheme for a quantitative flow evaluation. The basis for the observational methods was the construction of a July-averaged wind velocity vector at each observational site and for several selected hours. The reported high degree of wind steadiness ensured that the averaged wind velocities represent typical daily July winds at each observational location.[2] Finally, it should be noted that over water bodies, both observational methods are likely to be deficient somewhat because of the absence of stations there.

Fig. 2 illustrates the flow pattern toward the termination of the nocturnal period, as estimated by the model (Fig. 2A) and by the two observational analysis procedures (Figs. 2B and 2C). To a large extent the three methods indicate similar flow characteristics: a land breeze along the coastal areas (perturbed somewhat by the Carmel Mountain), and the dominancy of the westerly synoptic flow over the inland mountains and along their lee sides. In contrast to the objective analysis, however, the model computations indicate nocturnal drainage along the eastern side of the JRV, rather than upslope flow. Such upslope flow, however, may be an artifact of the observational analysis scheme, because of the lack of measurements in that region. Comparison of the wind speeds at the coastal area shows that the predicted wind speeds (Fig. 2A) are somewhat stronger than analyzed (Fig. 2C). This disagreement is attributed partially to the fact that the model has not adequately considered the complicated urbanized area of the coastal strip and misrepresented the terrain effect on wind speed reduction. On the other hand, however, anemometers used at synoptic stations have relatively high thresholds (e.g., Moses, 1968) which generally result in an underestimation of reported light wind speeds, a fact that can lead to some underestimation of the relatively low nocturnal wind speeds by the objective analysis method.

Fig. 3 presents the flow patterns 3 h following sunrise, during the commencement of the daytime thermal-induced circulations. The three methods show resemblance of the evaluated flow patterns, with southwesterly flow along the coastal plain which veers westerly over the mountain tops (over the mountains the westerly flow is indicated by the observed and modeled analyses to dominate through most of the daytime hours). Additionally, easterly thermally induced upslope flows are indicated along the eastern lower regions of the JRV.

It is of interest to point out that the predicted wind speeds (Fig. 3A) over the Judean mountains are no-

[1] The ratio of the magnitude of the mean wind velocity to the mean wind speed.

[2] The simulated domain includes most of the stations incorporated in the observational analyses.

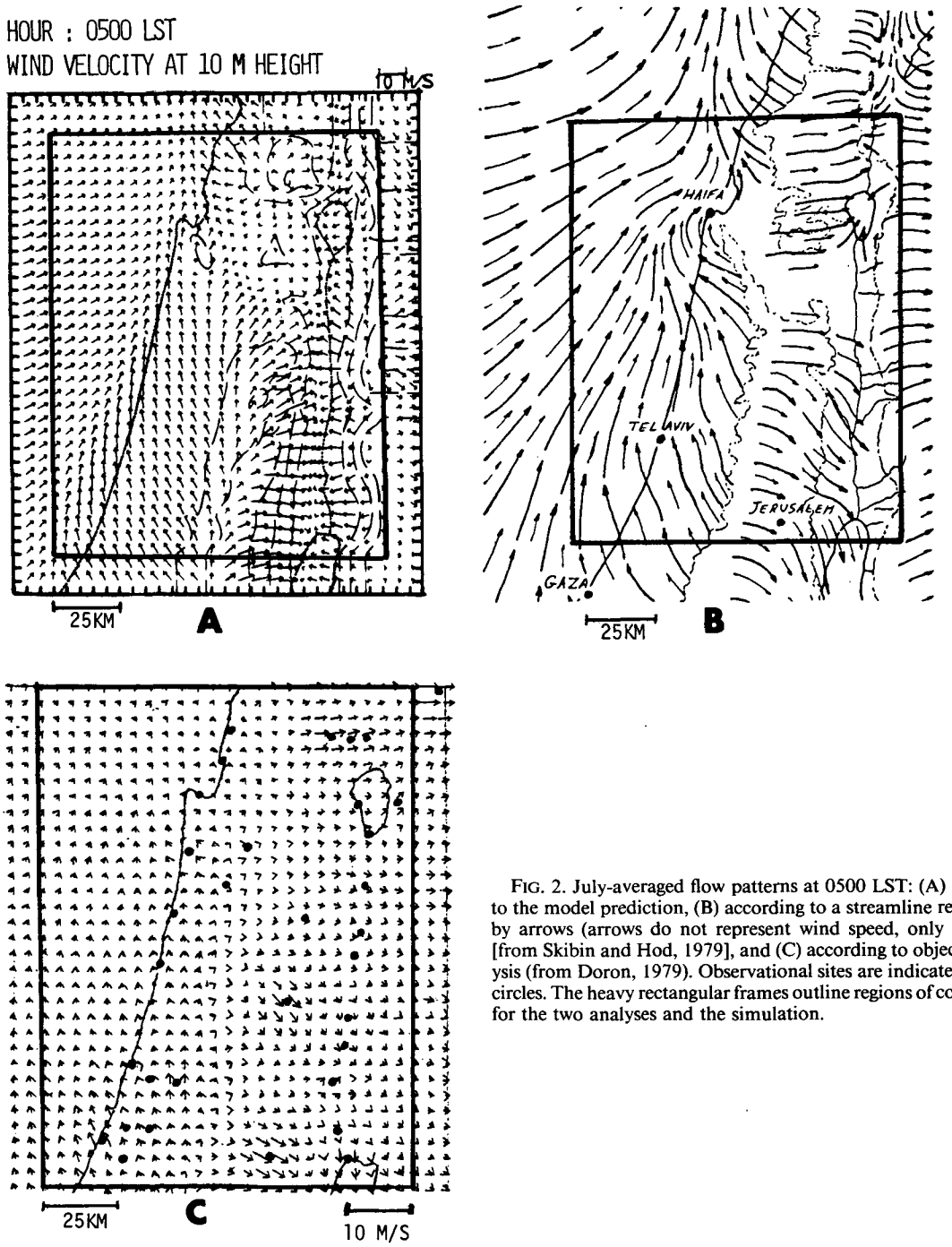

FIG. 2. July-averaged flow patterns at 0500 LST: (A) according to the model prediction, (B) according to a streamline represented by arrows (arrows do not represent wind speed, only direction) [from Skibin and Hod, 1979], and (C) according to objective analysis (from Doron, 1979). Observational sites are indicated by solid circles. The heavy rectangular frames outline regions of comparison for the two analyses and the simulation.

ticeably larger than in the objective analyses (Fig. 3C). Careful examination reveals, however, that at the two station sites which are located at the top of the mountains ridge (indicated by 1 and 2), the observed wind speeds are larger than those analyzed along the ridge line between both stations. This behavior is not expected since it is associated with a topography which is generally homogeneous in the north–south direction. However, in the absence of sufficiently dense observation sites along the mountain tops, the excessive weighting from contributions of stations located along the lower slope of the JRV results in an artificial reduction in the interpolated wind speed between the two stations. The examination of Fig. 5

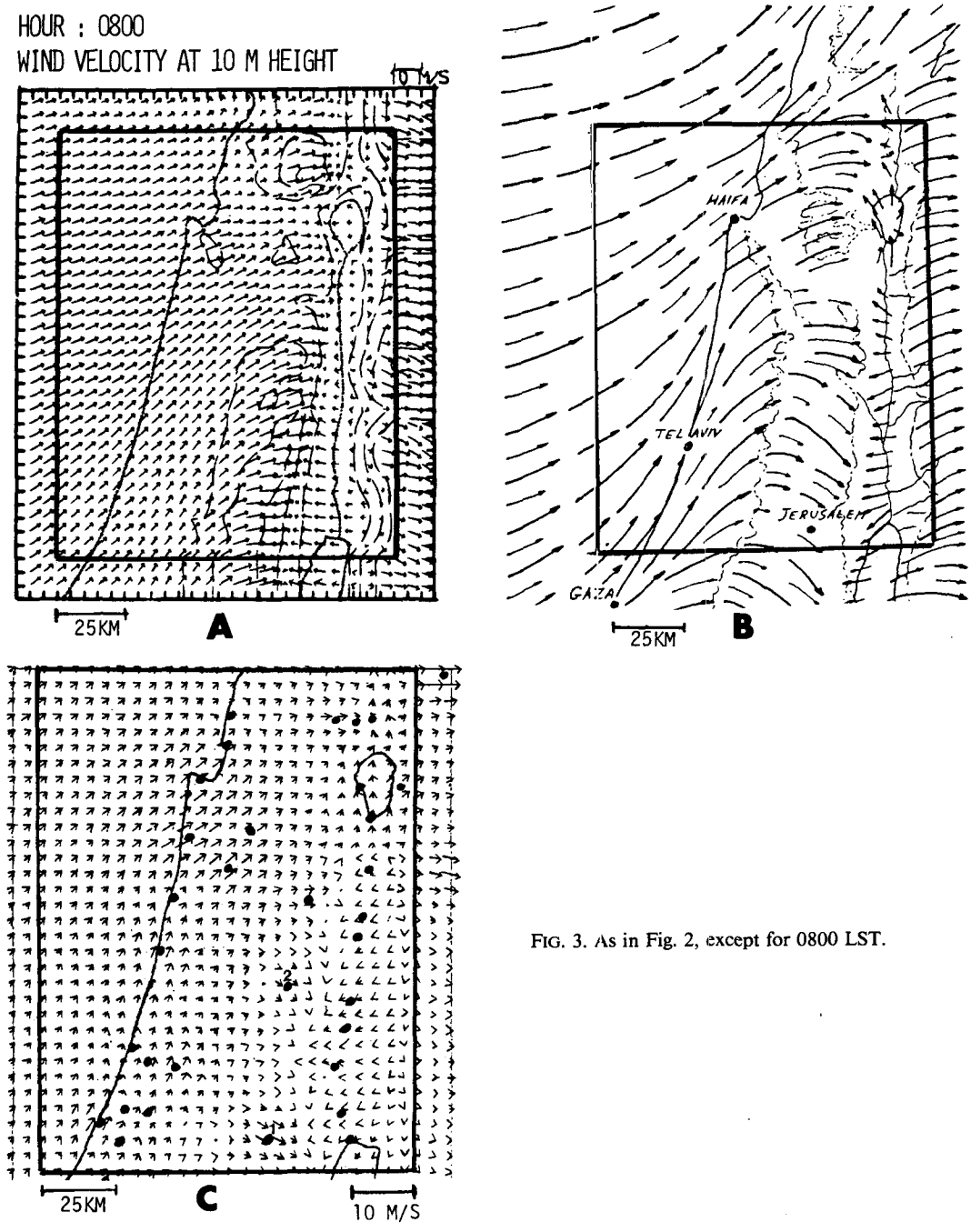

FIG. 3. As in Fig. 2, except for 0800 LST.

in Doron's paper, which is the same as Fig. 3C except for the elimination of most of the JRV stations, quantitatively illustrates this point. Thus, in view of this discussion, the model overprediction over the Judean mountains is actually smaller than indicated by the comparison with the objective analysis results in Fig. 3C.

The afternoon flow field is characterized by Fig. 4. The typical pattern during those times is the dominance of the Mediterranean sea breeze throughout most of the domain and its penetration to the JRV. At 1700 LST the sea-breeze-dominated flow acquired a northwesterly direction throughout the whole domain [the veering of flow from the southwest in the morning to the northwest in the afternoon results, as discussed, e.g., in Haurwitz (1947), from the effect of the Coriolis force on the intensifying sea breeze]. Generally, predicted wind speeds are similar to that estimated by the objective analysis, although the model-predicted wind speeds over the eastern Sea of Galilee

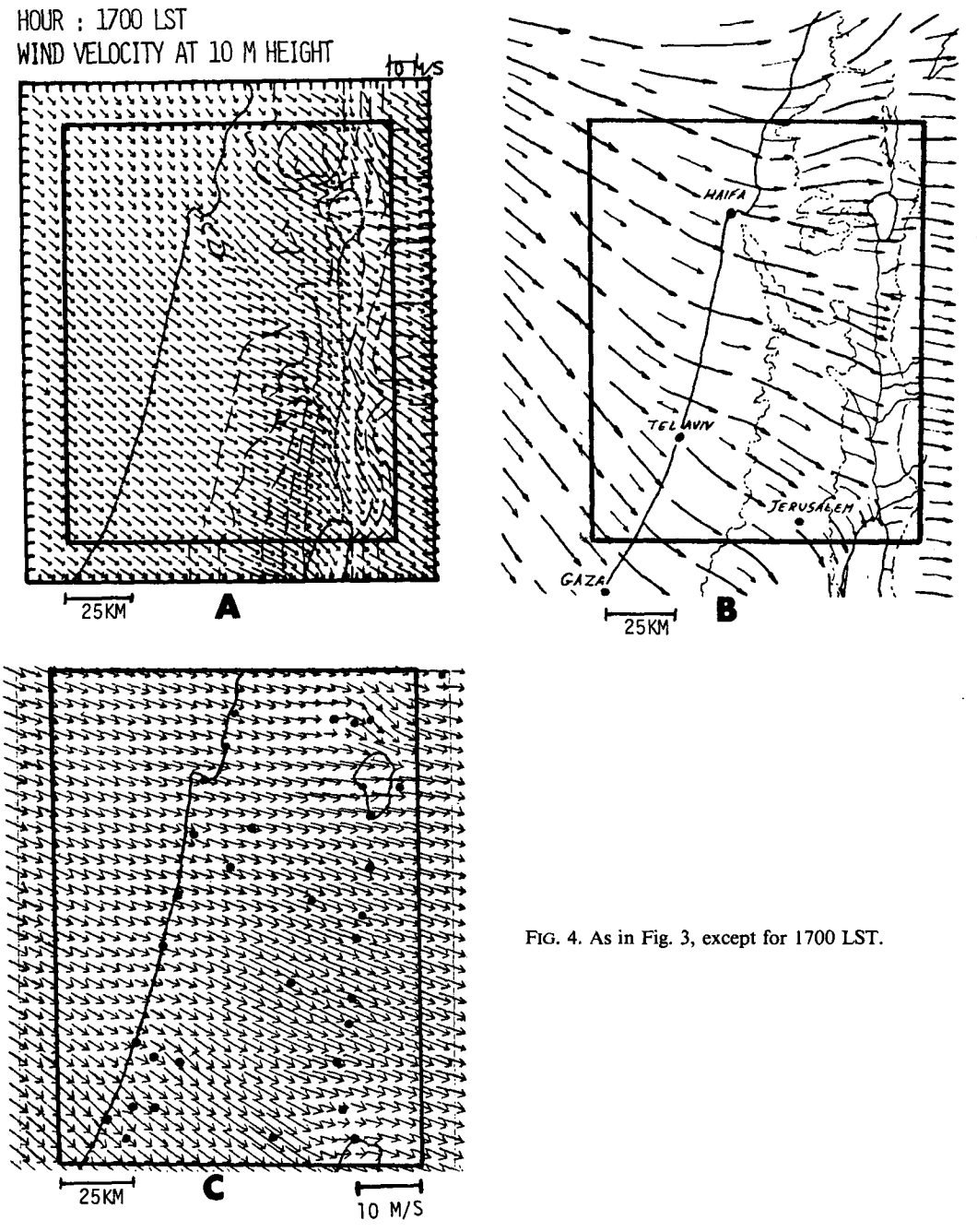

FIG. 4. As in Fig. 3, except for 1700 LST.

are underestimated when compared with the objectively analyzed wind speeds in that region. Such disagreements, perhaps, can be attributed to the smoothing of steep topography because of the relatively coarse model grid resolution, which is most pronounced in locations where the terrain requires sharp changes in the elevation gradient. Additionally, the presence of some time lag between the observed and predicted sea breeze inland penetration can also cause such a disagreement.

The comparison of the three methods for analyzing the July flow patterns over northern Israel for several selected hours, has indicated the following:

1) Generally, there is a reasonable agreement between the model-analyzed flow patterns and the other two methods.

2) The accuracy of the illustrated observational analyses is highly dependent on the density of the observational sites. Therefore, in subregions which lack wind data, mostly in mountainous terrain where local thermal-induced flows are typical, the observational analysis methods can have significant errors

(in the subjective analysis presentations these areas are either absent or drawn without observational justification).

3) Model flow pattern accuracy is highly dependent on the horizontal grid resolution (see, e.g., evaluations in Pielke, 1981); hence, local effects, smaller than the mesoscale, are not accurately simulated in the model.

b. *Temperature field*

The summer temperatures are highly correlated with the topographical evaluations and the eastward distance from the Mediterranean Sea. However, thermally induced circulations play a major role in modifying this pattern in some areas (*Atlas of Israel*, 1970). The 0500 and 1400 LST temperature patterns (which closely represent the daily minimum and maximum temperatures, respectively) are chosen for illustration. The 0500 LST predicted temperature distribution (Fig. 5A) indicates relatively high temperatures along the Mediterranean shore line due to the nearby warm water and at the JRV where the terrain is well below MSL.

The 1400 LST temperature pattern (Fig. 5B) indicates two regions of maximum temperatures along the east–west direction. They are located along the inner coastal plain and the JRV. The northern part of the JRV is affected at this hour by the descending Mediterranean sea breeze which causes some temperature increase due to adiabatic compression.

The largest disagreement between the predicted and observed temperatures in both the 0500 and 1400 LST patterns are found in stations located within the JRV. It suggests that finer model grid resolution is needed in order to accurately resolve the effects of the circulations due to the Dead Sea and the Sea of Galilee as well as to account for the irregular steep topography in this region.

In order to quantify the skill of the model representation of the temperature distribution over Israel, an error analysis has been performed. The root-mean-square error (RMSE), standard deviation of observed values (σ_{obs}), and standard deviation of predicted values (σ_{prd}) have been calculated. This analysis has been based on observed values for July 0500 and 1400 LST averaged temperatures, with 21 values from stations located in the coastal plain, and 33 values from sites in the mountainous area and in the JRV. The observed July averaged temperatures were gathered from *Climatological Normals* (1976) and from tables available in the Israel Meteorological Service. As dis-

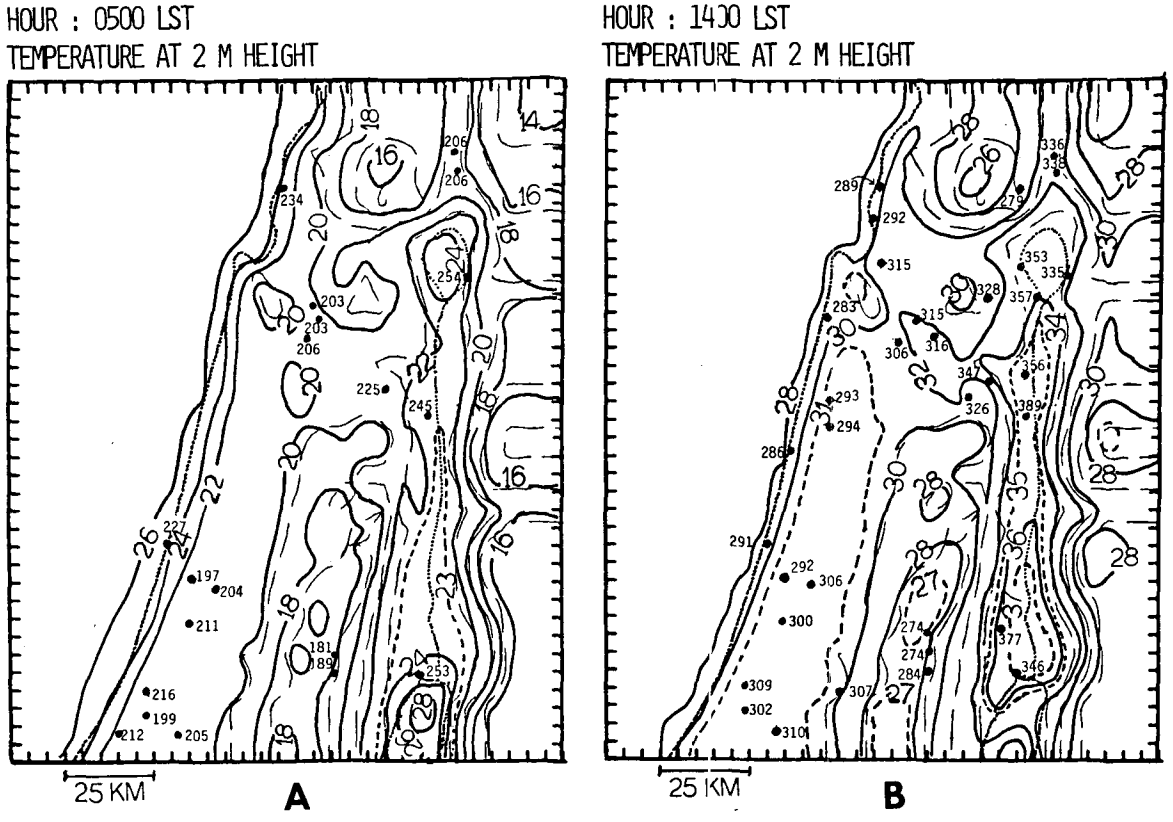

FIG. 5. The predicted temperature at 2 m height at 0500 and 1400 LST. Observational sites are indicated by solid circles. Observed temperatures (in units of 0.1°C) are given at the site markers.

TABLE 2. Model skill evaluation by means of standard deviation (σ) and RMSE.

	$\frac{\sigma_{obs}}{\sigma_{prd}}$	$\frac{RMSE}{\sigma_{obs}}$
1. Coastal stations	0.94	0.22
2. Mountainous stations	1.02	0.25
3. All stations	1.02	0.24
4. 16 stations (temperature change analysis)	1.04	0.52

cussed by Keyser and Anthes (1977), $\sigma_{obs} \approx \sigma_{prd}$ and $RMSE/\sigma_{obs} < 1$ indicate positive model prediction skill for the given sites. The calculated values for three stations groups as given in lines 1–3 of Table 2, indicate that these relations are satisfied separately for the coastal sites, the mountainous locations, and for all the available sites.

A more stringent test for the model skill involves the application of the above analysis to the predicted and observed changes of the temperature from the initial distribution. Such a skill analysis provides an evaluation of the skill of the model forcing as distinct from the ability of the model to represent the variations of the initial surface temperature distribution due to elevation change alone over the irregular terrain.

The data available were adequate to perform such an analysis where the 0500 LST temperatures were used for the initial values and compared against the skill of the 1400 LST predictions. This period of time reflects a large variation in temperatures, actually half of the daily temperature cycle. Based on 16 stations, the analysis was applied to the differences

$$\Delta T_{prd} = (T_{14} - T_{05})_{prd}, \quad (1)$$

$$\Delta T_{obs} = (T_{14} - T_{05})_{obs}. \quad (2)$$

Some relative reduction in model skill is indicated by this analysis (Table 2, line 4) although the model still shows skill in predicting the temporal variability of temperature.

6. Conclusions

Model-computed July wind patterns have been qualitatively compared with those obtained by two observational methods, while model skill for temperature evaluations have been quantitatively examined. Results indicate generally reasonable agreement between the model and observationally-evaluated regional climatology for those fields. However, the introduction of fine grid resolution in some regions (such as by utilizing nested grids) appears to be essential for further improvements in the spatial resolution of local climatology.

Since the simulated domain consists of highly irregular terrain, resulting in complex flow and temperature distributions, observational analysis should be regarded of high accuracy only in the vicinity of the available data sites. This accuracy can reduce sharply at relatively short distances from the observational sites, if there is no data support from additional sites, and the mesoscale gradients of these meteorological variables is large, such as, for example, along a coast or in highly irregular terrain (e.g., a cliff). On the other hand, the model is expected to be most useful at representing the general mesoscale pattern, rather than values at individual locations because of the limited spatial resolution of the numerical representation. Such models, however, can simulate regions of significant mesoscale gradients. Hence, using both modelling and observational methodologies for climatological studies can be of mutual complimentary benefit. The most useful contribution of the modelling approach can be in subregions where no observed data are available. The verification analysis results presented here also encourage using the current model as a tool for preliminary estimates of climatic patterns in other regions under similar persistent synoptic situations, when little meteorological data are available for observationally oriented climatological analyses.

Acknowledgments. We recognize the Atmospheric Sciences Section of the National Science Foundation under Grant ATM-8242931, and the Bi-National Israel-United States Science Foundation for their support in this study. Computer simulations presented in this study were performed at the National Center for Atmospheric Research, which is supported by the National Science Foundation. The authors wish to thank Eliahu Doron for providing them with his figures and Daniel Elbashan and Ronit Ben-Shara for the provision of temperature data. They would also like to thank Ann Gaynor, Sara Rumley and Verna Frick for their editing and typing.

REFERENCES

Anthes, R. A., and T. T. Warner, 1978: Simulation of mesoscale flows over Israel. *Israel Meteor. Res. Pap.*, Vol. II, Israel Meteor. Service, Bet-Dagan, 93–123.

Atlas of Israel, 1970: Survey of Israel, Ministry of Labour, Jerusalem.

Atwater, M. A., and P. Brown, Jr., 1974: Numerical calculation of the latitudinal variation of solar radiation for an atmosphere of varying opacity. *J. Appl. Meteor.*, **13**, 289–297.

Businger, J. A., J. C. Wyngaard, Y. Izumi and E. F. Bradley, 1971: Flux-profile relationships in the atmospheric surface layer. *J. Atmos. Sci.*, **28**, 181–189.

Clarke, R. H., 1970: Recommended methods for the treatment of the boundary layer in numerical models. *Aust. Meteor. Mag.*, **18**, 51–73.

Climates of the States, 1974: Water Information Center, Inc., Water Research Building, Manhasset Isle, Port Washington, NY 10500, 975 pp.

Climatological Normals, 1976: Ser. A., No. 3B, Israel Meteor. Service, P.O. Box 25, Bet-Dagan, Israel, 16 pp.

Deardorff, J. W., 1974: Three-dimensional numerical study of the

height and mean structure of a heated planetary boundary layer. *Bound.-Layer Meteor.*, **7**, 81–106.

Doron, E., 1979: Objective analysis of mesoscale flow fields—Israel and trajectory calculations. *Israel J. Earth Sci.*, **28**, 33–41.

Griffiths, J. F., and K. H. Soliman, 1972: *Climates of Africa. World Survey of Climatology*, Vol. 10, H. E. Landsberg, Ed., Elsevier, 75–132.

Haurwitz, B., 1947: Comments on the sea-breeze circulation. *J. Meteor.*, **4**, 1–8.

Keyser, D., and R. A. Anthes, 1977: The applicability of a mixed-layer model of the planetary layer to real-data forecasting. *Mon. Wea. Rev.*, **105**, 1351–1371.

Mahrer, Y., and R. A. Pielke, 1977: A numerical study of the flow over irregular terrain. *Beit. Phys. Atmos.*, **50**, 98–113.

——, and ——, 1978: A test of an upstream spline interpolation technique for the advective terms in numerical mesoscale model. *Mon. Wea. Rev.*, **106**, 818–830.

Moses, H., 1968: Meteorological instruments for use in the atomic energy industry. *Meteorology and Atomic Energy—1968*, U.S. Atomic Energy Commission, 257–300.

Nickerson, E. C., 1979: On the numerical simulation of airflow and clouds over mountainous terrain. *Contrib. Atmos. Phys.*, No. 52, 161–175.

O'Brien, J. J., 1970: A note on the vertical structure of the eddy exchange coefficient in the planetary boundary layer. *J. Atmos. Sci.*, **27**, 1213–1215.

Paegle, J., W. G. Zdunkowski and R. M. Welch, 1976: Implicit differencing of predictive equations of the boundary layer. *Mon. Wea. Rev.*, **104**, 1321–1324.

Pielke, R. A , 1974: A three-dimensional numerical model of the sea breezes over south Florida. *Mon. Wea. Rev.*, **102**, 115–139.

——, 1981: Mesoscale numerical modeling. *Advances in Geophysics*, B. Saltzman, Ed., Academic Press, 185–344.

Sasamori, T., 1972: A linear harmonic analysis of atmospheric motion with radiative dissipation. *J. Meteor. Soc. Japan*, **50**, 505–507.

Shaia, J., 1952: Upper air data for Beer-Ya'aqov. Ser. A., No. 19, Israel Meteorological Service, P.O. Box 25, Bet-Dagan, Israel, 38 pp.

Skibin, D., and A. Hod, 1979: Subjective analysis of mesoscale flow patterns in northern Israel. *J. Appl. Meteor.*, **19**, 329–338.